

PAPER • OPEN ACCESS

## Tree Detection with a Mobile Laser Scanner

To cite this article: A Masiero *et al* 2021 *IOP Conf. Ser.: Earth Environ. Sci.* **767** 012034

View the [article online](#) for updates and enhancements.



**ECS** The Electrochemical Society  
Advancing solid state & electrochemical science & technology

**239th ECS Meeting with IMCS18**

DIGITAL MEETING • May 30-June 3, 2021

Live events daily • Free to register

**Register now!**

# Tree Detection with a Mobile Laser Scanner

**A Masiero<sup>1,2</sup>, G Tucci<sup>1</sup>, A Vettore<sup>2</sup>**

<sup>1</sup>Dept. of Civil and Environmental Engineering, University of Florence, via di Santa Marta 3, Florence 50139, Italy

<sup>2</sup>Interdepartmental Research Center of Geomatics (CIRGEO), University of Padova, Viale dell'Università 16, Legnaro (PD) 35020, Italy

andrea.masiero@unifi.it

**Abstract.** Tree detection has been considered in a number of forest-related applications, mostly related to the need of determining the presence and position of trees, and, in certain cases, the associated biomass. Most of the tree detection methods are typically based on the use of LiDAR surveys, and they often aim either at determining tree crowns or stems. This paper proposes the use of a low cost hand held device to acquire a good spatial description of the area close to the track reachable by the operator holding the acquisition device. Then, a tree detection method based on the local application of the Hough transform is presented. The performance of the system is checked in an area hit by the Vaia storm in 2018.

## 1. Introduction

Tree detection has a relevant importance in several forest-related applications [1]. Furthermore, including more information in the detection, such as distinguishing stems and leaves, can also be of some interest in certain cases, for example to improve biomass estimation.

This paper is focused in particular in the case of tree detection when dealing with natural hazards, causing forest damages, and hence requiring a quick response of decision makers in order to properly deal with the consequences of such hazards (and to prevent the bad consequences of such events, if possible).

More specifically, this work is mainly motivated by the need of developing an automatic tool for evaluating the damages caused by the Vaia storm at the end of October 2018 in the North-Eastern regions of Italy, in particular in the Veneto and Friuli Venezia Giulia regions. Vaia storm was characterized by very strong winds that caused the fall of millions of trees. As a side consequence, it also caused huge economic losses, mostly due to the significant wood price reduction, due to the sudden availability on the market of a huge amount of fir wood.

The need for assessing the overall amount of fallen trees caused by the Vaia storm motivated the airborne Light Detection and Ranging (LiDAR) survey of the area interested by such hazard. Indeed, LiDAR data have frequently been used for properly mapping vegetation, and, in particular, for biomass estimation in forests [2].

In the considered case, airborne LiDAR (at few points per square meter) can be used to determine, by comparison with a previously acquired survey, the tree variations, in particular checking the presence of new gaps (e.g. this kind of considerations typically involve both tree detection and computing proper digital terrain models [3], [4]).



Despite such strategy can be quite effective, the recent development of new lightweight LiDAR sensors, which can also be mounted on drones or used as hand-held or backpack mobile laser scanners, opens the possibility of conveniently use such kind of technology to compute surveys of the area of interest at very high spatial resolution (comparable to that of static terrestrial laser scanning [5]).

The availability of high spatial resolution surveys allows to implement algorithms able also to determine several tree features, and, in particular, to detect which ones are fallen trees.

A number of works have been published considering the problem of tree detection. Most of such works are based on the use of airborne LiDAR, which clearly allows to quickly cover large areas.

Standard tree detection algorithms are often based on the detection of local maxima in canopy height models, watershed segmentation [6], and, in certain cases, such kind of segmentation procedure extended to hierarchical approaches [7], [8]. Other approaches, based on graph segmentation, such as normalized cut, has also been considered, when spatial point density is quite high [9]. Segmentation based on level sets methods may be useful as well [10].

The deployment of methods based on full-waveform LiDAR data has also been considered [11], however, such methods are clearly restricted only to the cases when a full-waveform LiDAR sensor is used. More recently, machine learning and deep learning methods have been successfully deployed in several detection and recognition applications (also related to point cloud processing) [12], hence they can be considered as promising tools also for the application considered in this paper.

The reader is referred to [13], [14] for a (benchmark and a) performance comparison between the different methods proposed in the literature for airborne LiDAR data.

Tree detection approaches based on the detection of tree features, such as the stem, has also been recently considered, for instance based on geometric features, e.g. cylinder fitting [15], when the spatial resolution of the dataset is sufficiently high.

Despite in certain cases spatial point density can be quite high also in airborne LiDAR data [9], such working condition is much more common in terrestrial (static and mobile) laser scanning (TLS and MLS, respectively), and in (the more recently developed) Unmanned Aerial Vehicle (UAV) LiDAR surveys.

Consequently, approaches based on geometric feature detection are much more common in datasets provided by TLS [14], MLS [16] and UAV-LiDAR [17]. Other spatial statistical methods may also be considered to properly detect objects, as done for instance in image processing [18].

Recently, UAV photogrammetric point clouds and hyperspectral imaging have also been effectively considered for tree detection [19].

An emerging approach [20], in particular for forest inventories, is that of using mobile platforms, such as backpacks [21], and in certain cases even smartphones [22].

In analogy with such works, this paper considers the use of a mobile, hand held, device. In particular, the hand held mobile laser scanning approach considered in this paper has been developed by deploying low cost sensors, in such a way to limit the cost of such tool to less than \$ 2k.

This paper aims at presenting the preliminary results obtained testing such device on the tree detection problem, and, more specifically, on checking its usage on the Marcesina plateau, which is part of the area hit by the Vaia storm. Figure 1 and 2 show examples of the current status of such area: the percentage of fallen trees is very high on the areas hit by the Vaia storm, several of them are still there (Figure 2), whereas some others have already been removed (central part of Figure 1).

## 2. Data Acquisition System

Data considered in this paper have been collected by means of the combination of a Livox Horizon LiDAR and an Emlid Reach M2 GNSS receiver (Figure 3).



**Figure 1.** Example of certain fallen trees in the area hit by the Vaia storm.



**Figure 2.** Example of certain fallen trees in the area hit by the Vaia storm.



**Figure 3.** Data acquisition system.

Livox Horizon is a low cost LiDAR sensor (\$ 800), principally designed for the use on autonomous vehicle applications. Livox Horizon acquires 240k points per second (480k points per second in dual return collection mode), with a 2 cm range precision (at 20~m distance from the LiDAR) and 280 m of maximum range. Field of view of the Livox Horizon is  $81.7^\circ \times 25.1^\circ$ . Interestingly, an Inertial Measurement Unit (IMU) is also embedded in the Livox Horizon, enabling the inertial data collection (sampling rate: 200 Hz).

Emlid Reach M2 is a multi-band multi-constellation GNSS receiver, initially developed for UAV applications. Its low cost (\$ 650, including receiver and antenna), low weight and small size make it a very convenient solution for employing it in mobile applications. Emlid Reach M2 worked in Network Real Time Kinematic (N-RTK) operative mode. According to the official receiver specifications, Emlid claims Kinematic positioning accuracy of:  $7 \text{ mm} \pm 1 \text{ ppm}$  horizontal, and  $14 \text{ mm} \pm 1 \text{ ppm}$  vertical.

The GNSS antenna has been attached on the top of the Livox LiDAR, whereas battery packs and

processing units, which mainly aims at storing all the acquired information (raw data are post processed to produce the final product), were positioned inside of a backpack, to be more easily carried by the operator. The system is clearly still in a early-prototype version (e.g. GNSS antenna is attached to the LiDAR just with some stick tape).

Overall, the weight of the hand held part of the system is about 1.2 kg.

Synchronization between Livox Horizon LiDAR and Emlid Reach M2 has been ensured by passing a GNSS-derived TTL synchronization signal as input to the LiDAR (by properly converting the Pulse Per Second (PPS) output of the Emlid Reach M2).

### 3. Case Study

The considered case study is part the area hit by Vaia storm on the Marcesina plateau, as previously mentioned. More specifically, given the clear difficulties in walking in the fallen tree area (see Figure 2), the system has been carried along the track shown in Figure 4 (black line).



**Figure 4.** Track walked by the operator carrying the acquisition system. The satellite view represents the area conditions before the Vaia storm.

Given the presence of several obstructions, mainly fallen trees and other vegetation, the real LiDAR visibility range is much less than the nominal 280 m. A more in depth investigation on this point is reported in Figure 5: despite some measurements can still be found at more than 150 m distance from the LiDAR, most of the measurements are collected in the 2-50 m range interval, which, given the difficulties in walking on the off-the-track area, means mostly mapping the area close to the track.

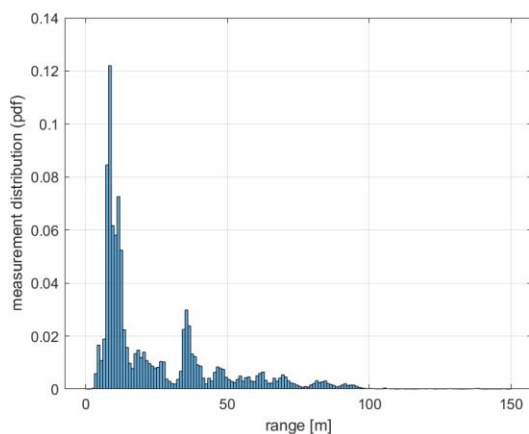


**Figure 5.** LiDAR measurement distribution as a function of the distance from the device.

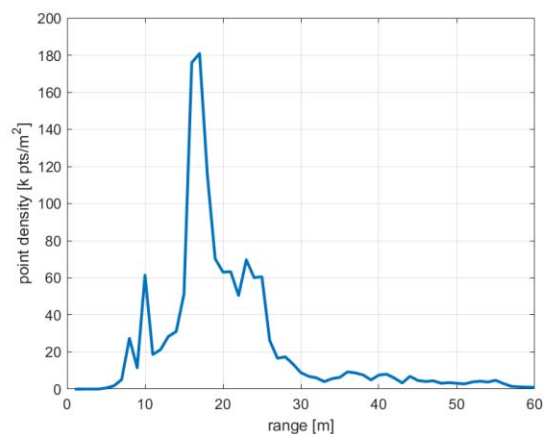


**Figure 6.** Measured point density as a function of the distance from the LiDAR.

The above considerations are confirmed by Figure 6 where the mapped (planar) point density is plotted as a function of the distance from the LiDAR. Figure 6 shows that the point density dramatically decreases for ranges larger than 30 m. Furthermore, Figure 6 also shows that the point density peak in the collected dataset is in the 15-18 m range interval, whereas a quite low point density can be observed

for ranges lower than 9 m: this is probably caused by the relatively small vertical field of view of the Livox Horizon LiDAR ( $25.1^\circ$ ), which during the acquisition was oriented mostly to map the scene (e.g. approximate horizontal orientation, in particular when oriented towards the damaged forest areas).

For what concerns the area quite close to the track, thanks to the very large number of points acquired by the Livox LiDAR per second, it is typically mapped at very high spatial resolution (as previously shown in Figure 6), however the real point density on an area depends also on the walking speed and on the device orientation changes.

It is also worth to notice that the measurement error of the acquired 3D points typically increases with the distance from the LiDAR device (the ranging error is already 2 cm at 20 m). From this observation and the one related to the point density (Figure 6), it is quite clear that in order to enable effective point processing procedures (e.g. to detect trees) it can be useful to impose a maximum range threshold to the points to be mapped (e.g. distance from the LiDAR device shorter than 30 m).

#### 4. Point Cloud Processing: Tree Detection

Tree detection in a specific area is obtained by means of a Hough transform approach, which can be repeated on several areas, if the region of interest is quite large.

Given a certain search area to be considered for detecting trees (both fallen or not), the tree detection algorithm is divided in the following steps:

- Consider the lists of  $\phi$  and  $\lambda$  angles to be investigated (Figure 7). In the approach implemented in this paper such lists were obtained by selecting an equally spaced set of values for both  $\phi$  and  $\lambda$ , where the variation between two successive considered angle values is of  $2^\circ$ . A couple of values ( $\phi$ ,  $\lambda$ ) identifies a potential direction of a tree.

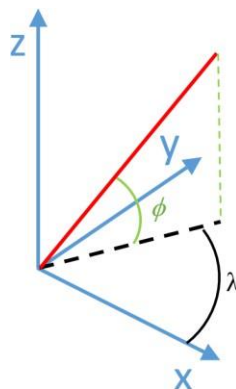


Figure 7. Definition of  $\phi$  and  $\lambda$  rotations.

- Assume that the overall region of interested is partitioned in several sub-areas, and that a tree to be detected should occupy a significant part of the length of a side of one of such sub-areas. Then, points within the considered sub-area are projected along each potential tree direction on a plane orthogonal to the considered direction.
- A discrete representation  $I_{\phi,\lambda}$  (raster-like) of the projected points is obtained by considering an equally spaced grid, with each square side of size  $\Delta s$ , where  $\Delta s=5$  cm in our implementation. In the obtained grid representation, each point is weighted proportionally to the local point spatial density in its neighbourhood (alternatively, a 3D box filter can be applied to the point cloud in order to produce a new cloud with homogeneous point density).
- A 2D filtering approach is used to speed up the detection procedure on each of such  $I_{\phi,\lambda}$ . To be more specific, several 2D circular ring filters are repeatedly applied to  $I_{\phi,\lambda}$ , aiming at detecting trees (with trunks approximated as cylinders of different radius) with trunk orientation along the  $(\phi, \lambda)$  direction. Hence, each of such filters will use a ring of different radius, whose value is related to the radius of potential tree trunks to be detected. Given the cloud point measurement noise, and the only

approximated description of a tree trunk as a cylinder, the considered circular rings have the average of the radius of the inner and outer circumferences corresponding to the ideal trunk radius  $r$ , but then, their real values are  $\Delta r$  far from  $r$  ( $\Delta r \approx 10$  cm in our implementation). The size of the used 2D cylinder filters is larger than  $2(r + \Delta r)$ : the 2D filter is defined in such a way that once applied on a location of  $I_{\phi, \lambda}$ , points falling on the ring are counted positively, whereas points falling within the size of the filter but outside of the circular ring are counted negatively. Overall, the 2D filter is zero mean, hence, if applied to a randomly uniformly distributed set of points, its result will be (approximately) zero everywhere.

- Local peaks on the 2D filtering outcomes are identified and, if their value is above a properly set threshold, set as detected trees. It is worth to notice that the local maximum condition should be checked both in the spatial and in the angular neighbourhood (e.g. also on  $I_{\phi', \lambda'}$ , for  $(\phi', \lambda')$  close to the  $(\phi, \lambda)$  associated to the hypothetical point of maximum).

The results of the detection procedure described above on the area shown in Figure 8 (a photo of the area is shown in Figure 8, whereas the corresponding point cloud is shown Figure 9, from approximately the same point of view) are presented in Figure 10.



**Figure 8.** Study area.

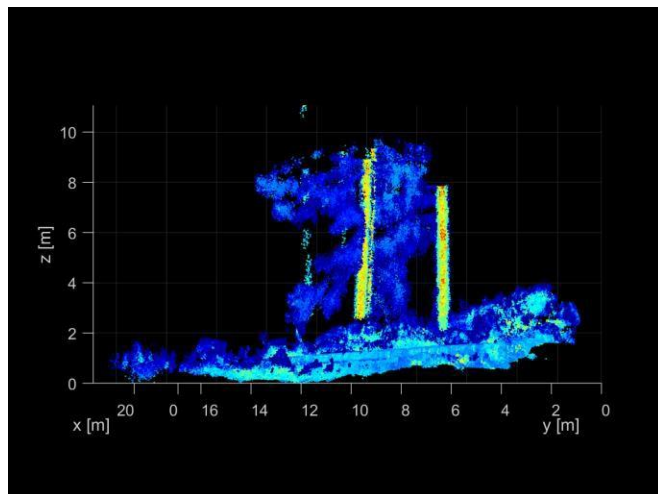


**Figure 9.** MLS point cloud obtained for approximately the same area shown in Figure 8.

Figure 10 clearly shows both the two detected fallen trees in foreground (almost overlapped, quite difficult to distinguish in Figure 8) and the three in the background.

Separating fallen trees from the other ones is clearly a quite easy operation: a quite reliable classification of the fallen trees among the detected ones can be simply obtained by checking if the value of the  $\phi$  angle associated to a tree is quite close to the angle of the ground slope in such location.

Such detected trees can be considered as the most visible ones in the point cloud, however, some others are at least partially present in the point cloud: the two fallen trees in the middle between those in foreground and those in background, whose view is partially obstructed by other vegetation.

Furthermore, also those more distant from the acquisition track have not been detected, but in this case the number of measured points describing them (if any) can probably be considered as insufficient to reliably detect a tree.

Points not related to trunks have been properly moved from the point cloud shown in Figure 10, as expected.

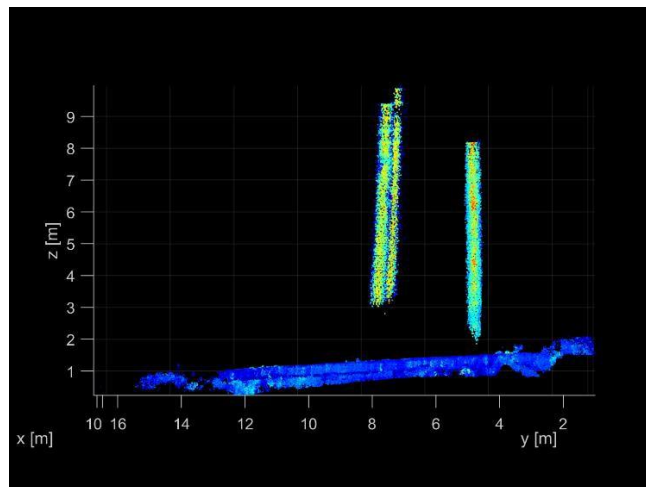


**Figure 10.** Point cloud obtained as a result of the proposed tree detection procedure in the area shown in Figure 7.

## 5. Conclusions

This paper proposed a hand held acquisition system, based on a low cost LiDAR, a GNSS receiver and an IMU, which can be used for instance to map the areas hit by natural hazards that are reachable on foot by an operator. Such system has been used to collect data in a region hit by the Vaia storm in 2018, and, a small test area has been considered to check the performance of a proposed processing method on the problem of tree detection in a point cloud. The GNSS receiver allowed to quite accurately acquire the track of the mobile laser (positioning error is expected to be of few centimetres), whereas the position accuracy of the acquired point cloud depends on the distance of the considered point from the LiDAR, and, in fact, the desired geometric quality of the obtained point cloud represents a limitation on the area that should be considered as properly mapped around the LiDAR. Despite a much larger area shall be considered to robustly test the performance of the detection approach, the preliminary results of Section 4 shows that such approach should be usable to properly detect also fallen trees, which is clearly an important goal in the considered application.

The main advantage related to the use of terrestrial mobile laser scanning in this kind of context is related to the possibility of mapping relatively quickly the areas close to the device track, and the high spatial resolution of the collected data. Nevertheless, among the terrestrial surveying methods, terrestrial static laser scanning is usually more reliable in terms of accuracy, whereas LiDAR mounted on drones shall be the a viable way for covering larger areas in less time, but at a much higher instrument cost.

The authors will consider in their future research work an extension of the presented system in such a way to enable effective mapping also in areas where GNSS is not reliable, exploiting both a LiDAR odometry-like approach [23] and the use of an external positioning system (e.g. based on ultra wideband ranging), which can be used independently of the GNSS [24].

## References

- [1] I. Sačkov, L. Kulla, and T. Bucha, “A comparison of two tree detection methods for estimation of forest stand and ecological variables from airborne LiDAR data in central european forests,” *Remote Sens.*, 2019.
- [2] F. Pirotti, G. Laurin Vaglio Laurin, A. Vettore, A. Masiero, and R. Valentini, “Small footprint full-waveform metrics contribution to the prediction of biomass in tropical forests,” *Remote Sens.*, vol. 6, no. 10, pp. 9576–9599, 2014.
- [3] K. Kraus and N. Pfeifer, “Determination of terrain models in wooded areas with airborne laser scanner data,” *ISPRS J. Photogramm. Remote Sens.*, vol. 53, no. 4, pp. 193–203, 1998.
- [4] M. Boreggio, M. Bernard, and C. Gregoretti, “Evaluating the differences of gridding techniques for digital elevation models generation and their influence on the modeling of stonydebris



- flows routing: A case study from rovina di cancia basin (North-eastern Italian alps),” *Front. Earth Sci.*, 2018.
- [5] A. Guarnieri, A. Masiero, A. Vettore, and F. Pirotti, “Evaluation of the dynamic processes of a landslide with laser scanners and Bayesian methods,” *Geomatics, Nat. Hazards Risk*, vol. 6, no.5–7, 2015.
- [6] L. Vincent, L. Vincent, and P. Soille, “Watersheds in Digital Spaces: An Efficient Algorithm Based on Immersion Simulations,” *IEEE Trans. Pattern Anal. Mach. Intell.*, 1991.
- [7] K. Zhao and S. Popescu, “Hierarchical Watershed Segmentation of Canopy Height Model for Multi-Scale Forest Inventory,” *ISPRS Work. Laser Scanning SilviLaser*, 2007.
- [8] P. Langfelder, B. Zhang, and S. Horvath, “Defining clusters from a hierarchical cluster tree: The Dynamic Tree Cut package for R,” *Bioinformatics*, 2008.
- [9] P. Polewski, W. Yao, M. Heurich, P. Krzystek, and U. Stilla, “Detection of fallen trees in ALS point clouds using a Normalized Cut approach trained by simulation,” *ISPRS J. Photogramm. Remote Sens.*, 2015.
- [10] A. Masiero, A. Guarnieri, F. Pirotti, and A. Vettore, “Semi-Automated Detection of Surface Degradation on Bridges Based on a Level Set Method,” *ISPRS - Int. Arch. Photogramm. Remote Sens. Spat. Inf. Sci.*, vol. 40, no. 3, pp. 15–21, 2015.
- [11] J. Reitberger, C. Schnörr, P. Krzystek, and U. Stilla, “3D segmentation of single trees exploiting full waveform LIDAR data,” *ISPRS J. Photogramm. Remote Sens.*, 2009.
- [12] M. Weinmann, B. Jutzi, S. Hinz, and C. Mallet, “Semantic point cloud interpretation based on optimal neighborhoods, relevant features and efficient classifiers,” *ISPRS J. Photogramm. Remote Sens.*, 2015.
- [13] H. Kaartinen *et al.*, “An international comparison of individual tree detection and extraction using airborne laser scanning,” *Remote Sens.*, 2012.
- [14] L. Eysn, N. Pfeifer, C. Ressler, M. Hollaus, A. Grafl, and F. Morsdorf, “A practical approach for extracting tree models in forest environments based on equirectangular projections of terrestrial laser scans,” *Remote Sens.*, 2013.
- [15] N. Pfeifer, B. Gorte, and D. Winterhalder, “Automatic reconstruction of single trees from terrestrial laser scanner data,” *Int. Arch. Photogramm. Remote Sens. Spat. Inf. Sci. - ISPRS Arch.*, 2004.
- [16] L. Zhong, L. Cheng, H. Xu, Y. Wu, Y. Chen, and M. Li, “Segmentation of Individual Trees from TLS and MLS Data,” *IEEE J. Sel. Top. Appl. Earth Obs. Remote Sens.*, 2017.
- [17] M. Wieser, G. Mandlbürger, M. Hollaus, J. Otepka, P. Glira, and N. Pfeifer, “A case study of UAS borne laser scanning for measurement of tree stem diameter,” *Remote Sens.*, 2017.
- [18] P. Facco, A. Masiero, and A. Beghi, “Advances on multivariate image analysis for product quality monitoring,” *J. Process Control*, vol. 23, no. 1, pp. 89–98, 2013.
- [19] O. Nevalainen *et al.*, “Individual tree detection and classification with UAV-Based photogrammetric point clouds and hyperspectral imaging,” *Remote Sens.*, 2017.
- [20] X. Liang *et al.*, “In-situ measurements from mobile platforms: An emerging approach to address the old challenges associated with forest inventories,” *ISPRS J. Photogramm. Remote Sens.*, 2018.
- [21] M. B. Campos *et al.*, “A backpack-mounted omnidirectional camera with off-the-shelf navigation sensors for mobile terrestrial mapping: Development and forest application,” *Sensors (Switzerland)*, 2018.
- [22] Y. Fan *et al.*, “A trunk-based SLAM backend for smartphones with online SLAM in large-scale forest inventories,” *ISPRS J. Photogramm. Remote Sens.*, 2020.
- [23] J. Zhang and S. Singh, “LOAM: Lidar Odometry and Mapping in Real-time, Robotics: Science and Systems, .,” *Robot. Syst.*, 2014.
- [24] A. Masiero, F. Fissore, A. Guarnieri, F. Pirotti, and A. Vettore, “Aiding indoor photogrammetry with UWB sensors,” *Photogramm. Eng. Remote Sensing*, 2019.